Egyptian Geophysical Society
EGS Journal, Vol. 20, No. 1, 51-65 (2022)

EVALUATION OF MINERAL POTENTIALITIES AS DEDUCED FROM AEROMAGNETIC AND AEROSPECTROMETRIC DATA FOR GABAL GATTAR AREA, NORTHERN EASTERN DESERT, EGYPT

S.H. Abd El Nabi[(1)], K.S. Farag[(1)] and A.M. Mohamed[(2)]

(1) Department of Geophysics at the Faculty of Science, Ain Shams University, Cairo, Egypt.

(2) MSc Student at the Faculty of Science, Ain Shams University, Cairo, Egypt.

تقييم الامكانات التمعدنية المستنبطة من البيانات المغناطيسية والطيفة الاشعاعية الجوية لمنطقة جبل جتار، شمال الصحراء الشرقية، مصر

الخلاصة: تقع منطقة جبل جتار بشمال الصحراء الشرقية بمصر جنوب غرب مدينة الغردقة حيث تعتبر هذه المنطقة من أهم المناطق لتواجدات اليورانيوم وتغطي المنطقة صخور الحمامات الرسوبية وجرانيت جبل جتار التي تتبع عصر البريكامبري الأعلي. ويتكون جرانيت جبل الجتار من النوع البرثيتيك الفاتح والكلسي قلي وجميعها من النوع التي تكون داخل اللوح. وتظهر التراكيب الجيولوجية علي صورة أنواع أولية وثانوية. وتمثل الطيات والصدوع والفواصل أهم التراكيب الثانوية. وتسود الصدوع الضاربة في اتجاهات شمال شمال شرق _جنوب جنوب غرب وهي تلعب دورا هاما في نقل المحاليل الحارة الغنية باليورانيوم. وقد تبين من دراسة العلاقة بين التراكيب الجيولوجية وتمعدنات اليورانيوم علي السطح او تحت السطح ان هذه التمعدنات توجد في نطاقات قص او تمزق داخل حوض تركيبي ناتج من قوي الشد والذي يصل طوله ٢ كم وعرضه نصف كم. وقد تم الوصول لهذه النتيجة بناء علي ربط النظام التركيبي بتوزيع تمعدنات اليورانيوم. وقد تم دراسة توزيع النشاط الاشعاعي في موقع جبل جتار وكذلك الظواهر التركيبية والجيولوجية والاشعاعية المرتبطة بها سواء علي السطح او تحت السطح. وقد أمكن تقسيم اليورانيوم بجبل جتار الي النوع العرقي لرواسب اليورانيوم. كذلك فان وجود تمعدنات اليورانيوم علي مستويات مختلفة يؤكد ترسب تلك التمعدنات من محاليل حارة صاعدة من خلال الفوالق الموجودة في الجرانيت.

وتمثل تلك الظواهر الي جانب حجم المواقع الحاوية لتمعدنات اليورانيوم احتمالات جيدة لوجود خامات اقتصادية لليورانيوم بمنطقة جبل جتار.

ABSTRACT: *Gabal Gattar area is situated in the northern Eastern Desert of Egypt, SW Hurghada city and is considered as an area of high potentialities for uranium deposits. The area is covered by Hammamat sediments and Gattarian granites. The Hammamat sediments are dissected by different types of dykes, while Gabal Gattar granites are cut only by basic dykes. These granites are mentioned as the younger pink granites, perthitic leucogranites, calc-alkaline and within plate granites. The granitic rocks are considered as one of the most essential sources for uranium deposits. The structural deformations of the study area are represented by primary structures and secondary ones. The most prevailing structures are folding, faulting and jointing. The faults, especially those trending in the NNE-SSW and N-S directions played as passways to the ascending uranium-bearing hydrothermal solutions carrying uranium mineralizations. Most of them are located within a large pull apart basin. It is found from the relation between structures and uranium mineralization within the highly promissing shear zones that uranium mineralizations are located within a large pull-apart basin, having about 2 km length and 0.5 Km width. Delineation and evaluation of mineral resources are most important exploration parameters required for investment decisions. Identifying the best probable sites for uranium mineralization in terrains of lack subsurface penetrations is a challenging task. In northern part of Egyptian Eastern Desert, the uranium occurrences of Gabal Gattar area are among the most important source of uranium mineralization. The famous uranium mineralization in this occurrence is restricted to the geological contact zone between the Hammamat sedimentary rocks and the G. Gattar Alkali feldspar granite. As well, molybdenite-rich granite samples were collected from Gabal Gattar granitic pluton which represents one of the most important molybdenum mineralized district in Egypt. The Gabal Gattar area has been investigated for uranium by the Nuclear Materials Authority of Egypt (NMA) with the exploration program which was created in 1984. G. Gattar area locates in the high mountainous terrains of the North Eastern Desert of Egypt (Fig. 1). The exploration efforts, carried out by the NMA at G. Gattar area, led to the discovery of more than twenty uranium occurrences in the northern parts of G. Gattar granite (Shalaby, 1990, 1996; Abu Zaid, 1995; El Zalaky, 2002; El Kholy el al., 2012). These occurrences were named, according to date of discovery as, G-I, G-II, G-III, G-IV, G-V…etc. (Fig. 2).*

The uranium mineralization at all these occurrences are related and confined to the granite itself but in G-V occurrence, uranium is restricted to the contact zone between Hammamat sedimentary rocks (HSR) and Gabal Gattar granite (Roz, 1994; Abdel Hamid, 2006)

1- INTRODUCTION

Location Of The Study Area

Gabal Gattar area lies in the northern part of the Eastern Desert of Egypt at the intersection of coordinate 27° 06' N and 33° 16' E, at a distance of 35 Km from Hurgada City, at the Red Sea Coast. The younger Gattarian granites cover about 2/3 of its surface area in an NE-SW direction (Fig. 3).

Petrography of the Gabal Gattar granites: Gabal Gattar granites represent the northern part of a large batholith of younger granites. These granites are predominantly formed of medium grained rocks varying in colour from pink to reddish pink in fresh samples and have tendency to turn pale pink to reddish brown due to alteration along shear zones (Salman et al., 1986).

El Rakaiby and Shalaby (1992) classified the rocks of this complex batholiths according to their mode of occurrenees and petrography into three phases: G1, G2 and G3.

Gabal Gattar pluton belongs to G3 phase which is the youngest of three phases. Granitic rocks are distinctive components of the continental crust and can be divided into S-, I-, M- and Atypes based on chemical features. The term “A-type” refers to anorogenic, alkaline and anhydrous granitoids. Different models are proposed for the formation of A-type granites: 1) fractionation of mantle-derived magmas, 2) partial melting of various crustal sources with variable contamination from mantle-derived magmas, and 3) lower-crust metasomatism by alkalirich mantle-derived fluids leading to fertilization and melting of the crust. A-type granitoids can be subdivided into two groups based on multi-trace element ratios: 1) type A1, related to sources similar to those of oceanic island basalt (OIB), and 2) type A2, related to sources originally formed type A2, related to sources originally formed by partial melting of lower crust through subduction or continent–continent collision (post-orogenic setting). The geographically southern part of Gabal Gattar batholiths (light pink to pink granite) is dominated by syenogranite and the northern part (red granite) mainly comprises alkali-feldspar granite . They are dominantly composed of alkali-feldspar, quartz, plagioklase and biotite (Mahdy et al., 2015). represents diagram of modal quartz (Q), alkali-feldspar (A), and plagioclase (P) with marked Gabal Gattar granites composition by brown color.

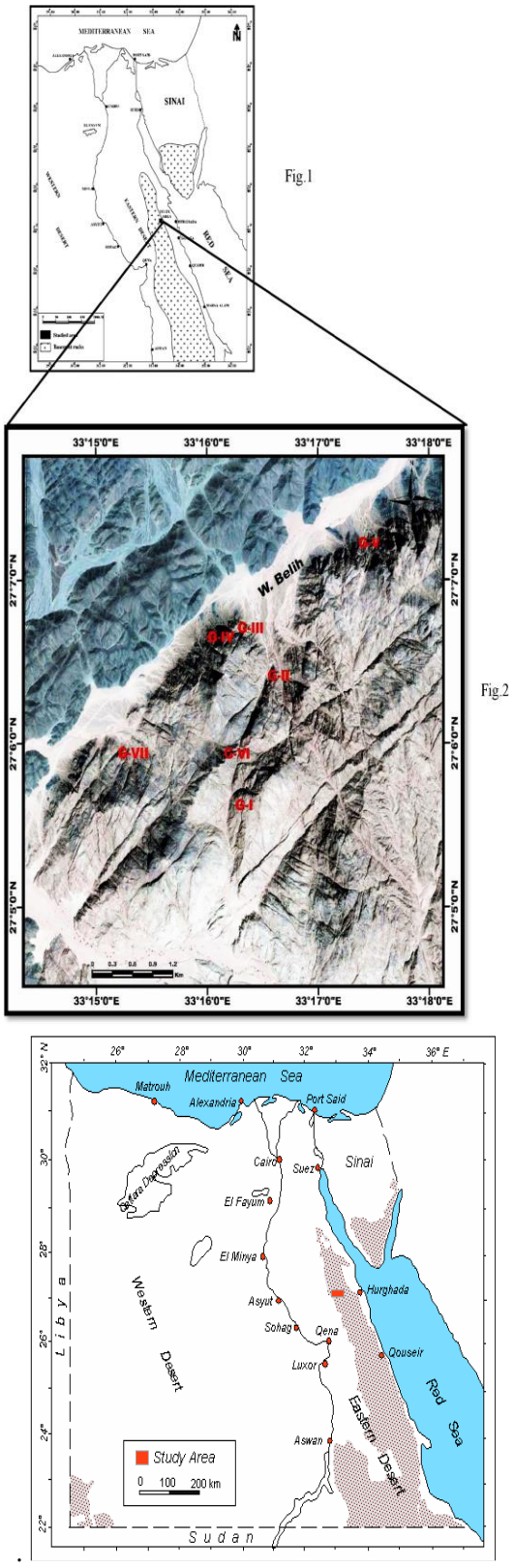

Fig. (3): Location map of the study area.

Geologic Setting

The area of G. Gattar mainly comprises basement rocks of Precambrian age mainly represented by the old Hammamat sediments of molasses type and the younger pink granites.

The Hammamat sediments are slightly metamorphosed. They contain polymictic conglomerates derived from the pre-existing diorites, granodiorites, mafic and felsic volcanic elastics. The fine Hammamat sediments include greywackes, sandstones, slates and siltstones. Generally,the Hammamat sediments are deposited in discontinuous intermounataineous basins as a result of an alluvial fan braided stream complex [1]. On the other hand, Stern et al., [2] suggested that the deposition of Hammamat sediments, in the northern Eastern Desert, was in down faulted grabens nearly trending NE-SW. It was reported that the age of the Hammamat sediments in the N.E.D. is bracketed between the Dokhan volcanics (59a ± 13Ma) and the Gattarian granites (57S Ma) [3].

Gabal Gattar granites represent the northern part of a large batholith of younger granites. El Rakaiby and Shalaby [4] classified the rocks of this complex batholith according to their mode of occurrenees and petrography into three phases named; Gl, G2 and G3. Gabal Gattar pluton belongs to G3 phasewhivh is the youngest. The contacts between the granites and the Hammamat sediments are usually sharp with slight metamorphism in these sediments. Gabal Gattar granites are predominantly formed of medium grained rocks varying in colour from pink to reddish pink in fresh samples and tend to turn pale pink to reddish brown due to alteration along shear zones. the commonest alterations in these granites are hematitization, silicification, episyenitization, fluoritization kaolinization and epidotization besides the frequent presence of manganese dendrites and carbonates.

Under the microscope, Gabal Gattar granites are perthitic leucogranites essentially composed of a nearly equal amount of quartz and potash feldspars in addition to plagioclase, minor amount of biotitc and few muccovite. The occessory minerals are zircon, fluorite, apatite and opaques such as sphalerite, chalcopyrites, pyrite, hematite and magnetite.

The geochemistry of Gabal Gattar granites have been studied by Stern and Gottfried [5]. They mentioned that these granites are characterized by their high silica, enrichment in total alkali contents, low to moderate alumina, low contents of CaO, MgO, total iron and titanium. Gabal Gattar granites have many common features with Group II Egyptian younger granite of Greertberg (1981) and the Group III younger granitoids of Saudi Arabia [6].

The emplacement of the younger granites of the Arabo - Nubian Shield was associated with diffuse extension and / or strike slip shear movements that follow the collisional events by about 25 to 75 Ma and are compositionally close to the "within plate granites" (Sylvester, [7].

Attawiya [8] added that the magma of Gabal Gattar granites is of calc-alkaline type with some alkaline affinity and the trace element data showed that its magma had evolved in a within plate anorogenic environment.

The area is subjected by metavolcanics, diorite, Hammamat sedimentary rocks, felsites dykes, younger granites and post granitic dykes of basic composition . G. Gattar is dissected by different sets of faults and fractures striking in NE-SW, NW-SE, NNE-SSW and ENE-WSW (Fig. 4). Its age is assigned by Hashad (1980) to be 484 Ma. According to Hussein et al., (1982) classification ofthe Egyptian granites, it is referred to as "G3-granites".

The potential area in the northern sector of G. Gattar batholiths comprises several promising occurrences namely: GI, GII, GVI as intragranitic type and GV as paragranitic types or contact type uranium mineralization. The main rocks covering this part are Hammamat sedimentary rocks, younger granite and post granitic dykes.

The recorded mineralized occurrences are controlled by NNE-SSW and its intersection with ENE-WSW and NW - SE.

The Hammamat sedimentary rocks comprise conglomerates, graywackes and siltstone. They are of molasse type, were deposited in intermountain basins, as a resuit of rapid uplift and erosion in fresh Water braded stream and alluvial environment (Grothaus et al, 1979).They are intruded by the younger granite of G. Gattar in sharp intrusive contact.

Surface and subsurface works were caried out at Gl occurrence: they are composed of a main adit (425 m) and three cross cuts or drifts. Dl (53.23 m.), D2 (41.8 m.) and D3 (36.2 m.). The aim of these works was to follow up the surface structures controlling the uranium mineralization in depth and to study the behaviour, mode of distribution and the related alteration features at deeper levels. Geology of Uranium Mineralization.

Through the last few decades, many uranium occurrences have been revealed in the Eastern Desert by the Egyptian Nuclear Materials Authority. Gattar granites are regarded as one of these occurrences, where surficial uranium mineralization was discovered by Salman et al. (1986). A few years later, several uranium occurrences within the same area have been identified (Roz, 1994; Nossier, 1996; and Shalaby, 1996).

Uranium mineralization is mainly restricted to sheared tectonic contact between Gattar granites and the older Hammamat sediments. The Role of Argillic Alteration in Uranophane Precipitation.

49 associated NE-SW and NNE-SSW faults and shear zones represent a pathway for the hydrothermal fluids, creating conditions favorable for alteration of Gattar granites, e.g. dissolving quartz, muscovitization,

argillization and carbonitization. The mineralization, in the form of stains along crevices and fracture surfaces (Mahdy et al., 1990), is best hosted in the Hammamat sediments near contact with sheared Gattar granites.

A number of mineralization may, however, occur in the hydrothermally altered parts of Gattar granites and localized within several shear and fractured zones that are filled with quartz veins (Salman et al., 1986; Helmy, 1999; and El-Kammar et al., 2001). Void-filling calcite have been observed in Gattar granites. Fluorite is found in significant amounts as subhedral transparent crystals. The majority of these crystals are commonly violet with blue shades. The color may reach black especially in the composite grains of fluorite and secondary uranium minerals.

The background values of uranium and thorium in the unaltered rocks range from 4.9 to 9.8 ppm U and 15 to 21 ppm Th for granites and from 5.4 to 41 ppm U and 2.8 to 6.4 ppm Th for the sediments (El-Kammar et al., 2001). These values increase in altered varieties, particularly the siltstones of the Hammamat sediments, where average U reaches 4284 ppm with low Th values (average 7 ppm). Sayyah and Attawiya (1990) reported the presence of uraninite as a main primary uranium mineral in the granitic rocks. However, primary U-ores in the mineralized shear zone have not been evidenced at the surface in the recent work (e.g. El-Kammar, et al., 2001; and Dawood, 2003), as well as the present study.

The secondary uranium minerals, represented mainly by uranophane, is detected as patches and fracture-fillings in both sheared Gattar granites and hematized Hammamat sediments (Dawood, 2003). It forms well developed needle and radiated crystals. Its color ranges from lemon yellow to straw yellow. Uranophane crystals are a few millimeters in size and occur as separate crystals or precipitated on clay minerals.

Structures

The primary structures, in the study area, are mainly expressed by bedding, graded bedding, cross bedding and ripple marks. Secondary structural elements are folds, joints and pull-apart basins

- Folds

Generally, the bedding of the Hammamat sediments is nearly horizontal to slightly dipping to the SE direction along the northern bank of Wadi Um Elbalad and moderately dipping to SE in the area between W. Um El Balad and Wadi Balie . It is relatively steeply dipping between Gabal Gattar granites and the Hammamat sediments along the southern bank of Wadi Balie. Some minor asymmetrical anticlinal and synclinal folds are recorded with axes plunging 15° to 30° to the WSW direction.

- Joints

The most major surface and subsurface trends of joints in Gabal Gattar granites are the NNE-SSW and N-S both forming about 36% of the total measured joints. The next predominant trends are the NE-SW, WNW-ESE and NW-SE. The less abundant trends are the NNW-SSE, ENE-WSW and E-W respectively.

The uranium surface and subsurface mineralized joints at GI uranium occurrence predominate the N-S, NNE-SSW, NW-SE and NE-SW dirtection. Although the NNW-SSE and ENE-WSW joint trends are less abundant both in surface and subsurface, they are of the most important trends scheming the uranium mineralization when intersecting with the predominant trends.

- Faults

A big number of fault trends were measured in the studied area . their distribution and profusion are as follows:

- The predominant trends: NNE-SSW (19.54%) and NNWSSE (17.73%).
- The abundant trends: N-S (15%) and NW-SE (14.55%.
- The common trends: NE-SW (12.73%) and WNW-ESE (11.81%).
- The less common trends: E-W (4.55%) and ENE-WSW (4.09%).

The NNE -SSW faults are mainly sinistral while the NW-SE ones are mostly dextral. They both represent two complementary sets of shear fractures dominating in the Gulf of Aqaba and the Gulf of Suez particularly.

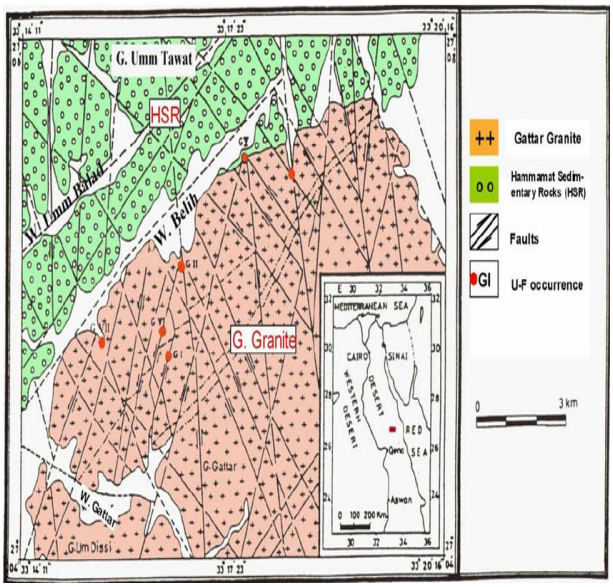

Fig. (4). Map of G. Gattar area. Geological – structural.

- Pull Apart Basins

Keary et al. |4] mentioned that where the curvature of strike - slip fault is pronounced or where one fault terminates side step to an adjacent parallel fault, the curved zone or area separating the faults is thrown into tension provides arise to an extensional trough known as

a pull apart basin. Pull apart basins are now recognized as being important sites of mineral resources.

In the study area of Gattar, pull apart basins are noted in both Hammamat sediments and the Gattarian granites. Their sizes are varying from few centimeters to hundreds of meters. The major and important pull apart basin is that including GI, Gil and GVI uranium occurrences which represent two subparallel shear zones where the granites are highly altered and hematitized.

The uranium mineralizations along these shear zones are in the orm of numerous disconnected lenses ranging in size from 0.5 x 0.5 m. to 100 x 5m., mostly accompanied with strong hematitizations, silicifications and abundant deep violet fluorite. The formed pull-apart basin by these two shear zones is an "S" shape one and have length width ratio is 3, (Fig. 5).

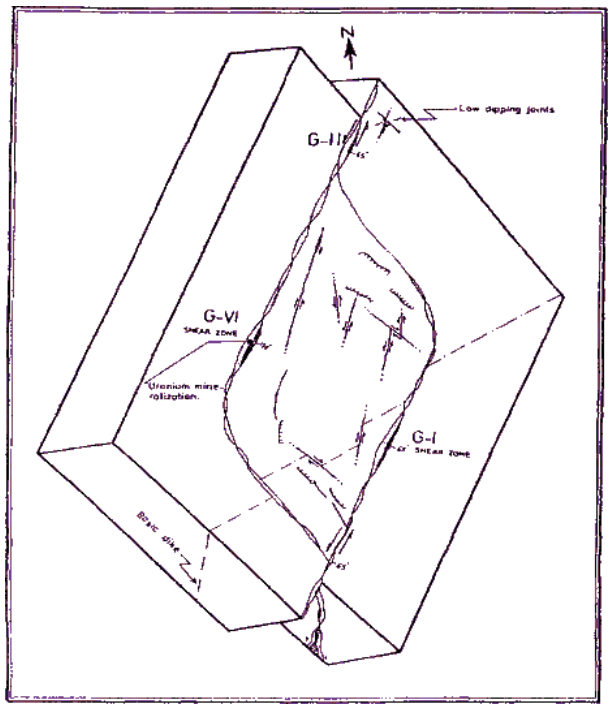

Fig. (5) : Sketch map of the large pull-apart basin controlling the distribution of uranium mineralization in G-I, G-H and G-VI,G. Gattar prospect.

Aerro-Spectrometric Survey

General

Airborne Radiometric (Gamma Ray Spectrometry) Surveys

Radiometric surveys detect and map natural radioactive emanations, called gamma rays, from rocks and soils. All detectable gamma radiation from earth materials come from the natural decay products of only three elements, i.e. uranium, thorium, and potassium. In parallel with the magnetic method, that is capable of detecting and mapping only magnetite (and occasionally pyrrhotite) in soils and rocks, so the radiometric method is capable of detecting only the occurrence of U, Th, and K at or near the surface of the ground.

Qualitative interpretation

Total count map

Investigation of the total count map (Fig. 7) shows that, it can be divided into three distinct levels. The first low radiometric concen-tration level is less than 37 Ur and recorded at the northwestern, that is covered by hammamat sediments.

The second level ranges from 66 to 129 ur and recorded mainly over pink granite , granodioritic and metavolcanic at the northeastern and dis-persed spots in the central parts of the area. The third level is more than 134 ur and recorded over the red granitic rock south part of the study area.

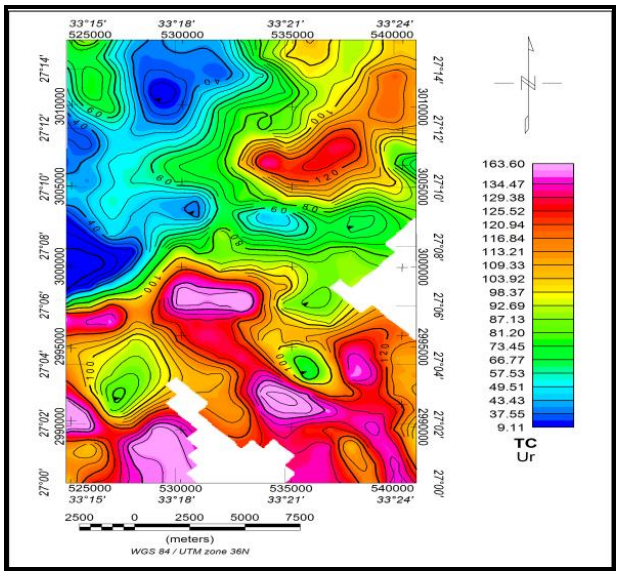

Fig. (7): Fill coloured contour map of Total Count (T.C) in Ur Gabal Gattar area, North Eastern Desert, Egypt.

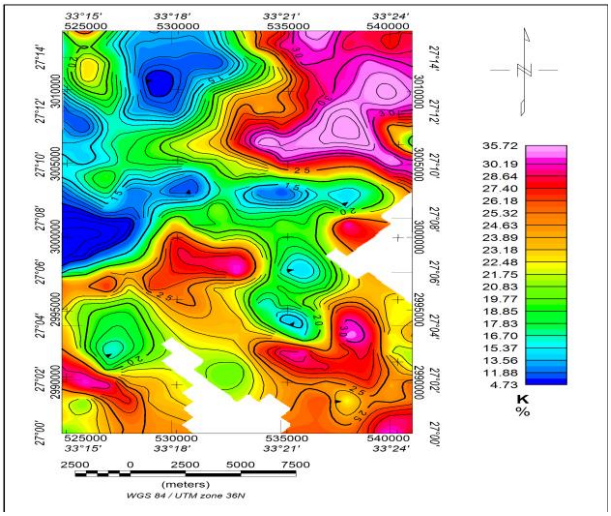

Fig. (8): Fill coloured contour map of Potassium (K) in %, Gabal Gattar area, North Eastern Desert, Egypt.

Potassium is a radioactive element, identified by the chemical symbol K. Under normal circumstances it is by far the most abundant naturally happening radioactive element within the human body.

Radioactive potassium-40 is only a tiny fraction of all the potassium present in nature but because potassium is one of the ten most abundant elements on Earth, it is the largest source of natural radioactivity in humans and animals.

The values of potassium concentrations can be divided into three levels of concentrations. The lowest level (less than 11%) is associated hammamat sediments. The values ranging from (13–28%) are represented the intermediate level and associated with pink granite , granodioritic and metavolcanic. The third level is the highest zone (more than 30%) and is recorded over red granite of the studied area.

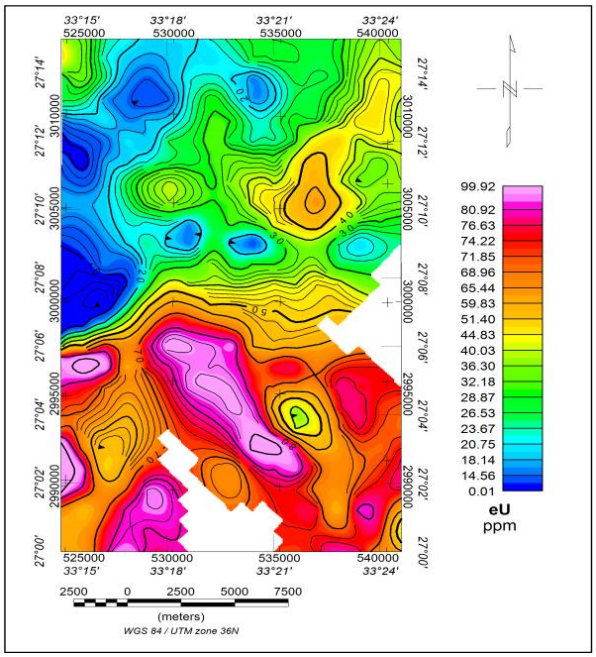

Fig. (9): Fill coloured contour map of equivalent Uranium (eU) in ppm, Gabal Gattar area, North Eastern Desert, Egypt.

Uranium is a naturally occurring metallic element that has been present in the Earth's crust since formation of the planet. Similar to many other minerals, uranium was deposited on land by volcanic action, dissolved by rainfall, and in some places, carried into underground formations. In some cases, geochemical conditions resulted in its concentration into "ore bodies." Uranium is a frequent element in Earth's crust (soil, rock) and in seawater and groundwater.

Uranium has 92 protons in its nucleus. The *isotope2* 238U has 146 neutrons, for a total atomic weight of approximately 238, making it the highest atomic weight of any naturally occurring element. It is not the most dense of elements, but its density is almost twice that of lead.

The equivalent Uranium (eU in ppm) contour map (Figure 9) shows three different levels of uranium concentration values. The highest level (more than 77 ppm) is correlated mainly with red granite in the south part of the map .The intermediate level ranged from 26 to 74 ppm and associated mainly with pink granite , granodioritic and metavolcanic .The lowest level is less than 20 ppm and associated with the hammamat sediments.

The element thorium was discovered in 1828. More than a 100 years later, in 1941, its potential as an energy source was proved. Thorium is estimated to be three to four times more plentiful than uranium in the Earth's crust and it is one of the most energy dense elements found in nature. The element has some favorable uniqueness making it an ideal nuclear fuel for next generation reactors; it is safe, clean, affordable and scalable. You can hold your whole lifetime's energy need in the palm of your hand.

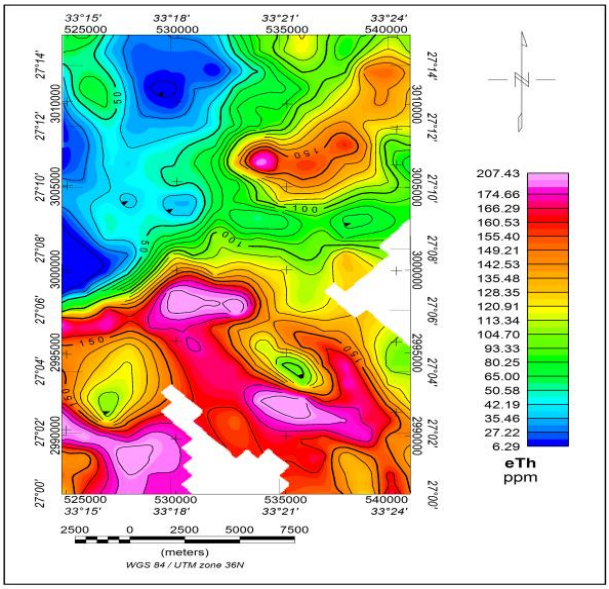

Fig. (10): Fill coloured contour map of equivalent Thorium (eTh) in ppm, Gabal Gattar area, North Eastern Desert, Egypt.

The equivalent thorium (eTh in ppm) contour map (Figure 10) is divided into three levels of thorium concentrations. The lowest level associated mainly with hammamat sediments and having values less than 42 ppm. The intermediate level ranged from 53 to 165 ppm and recorded over pink granite , granodioritic and metavolcanics. The highest level (more than 174 ppm) is related to red granite.

The equivalent (eU /k) contour map (Figure 11) shows three different levels of concentration values. the highest level (more than 3.4) is correlated mainly with red granite in the south part of the map. The

intermediate level ranged from 1.2 to 3.2 and associated mainly with pink granite , granodioritic and metavolcanic .The lowest level is less than 0.9 and associated with the hammamat sediments.

The equivalent (eU /eTh) contour map (Figure 12) shows three different levels of concentration values. The highest level (more than 0.63) is correlated mainly with red granite in the southeastern and nortwestern parts of the map .The intermediate level ranged from 0.34 to 0.57 and associated mainly with pink granite , granodioritic and metavolcanic .The lowest level is less than 0.27 and associated with the hammamat sediments.

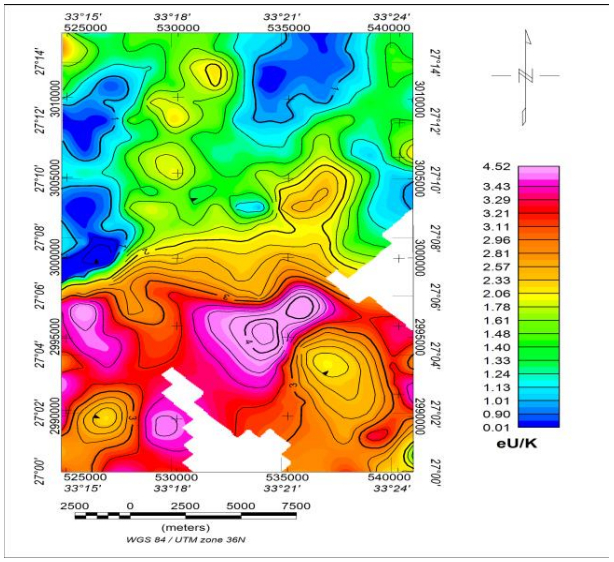

Fig. (11): Fill coloured contour map of equivalent (eU /k) , Gabal Gattar area, North Eastern Desert, Egypt.

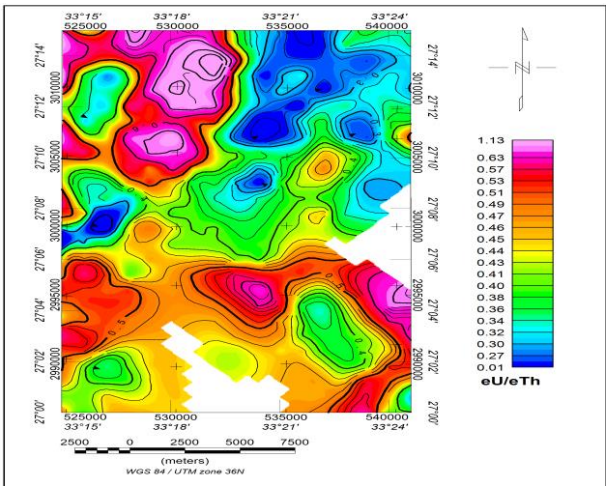

Fig. (12): Fill coloured contour map of equivalent (eU /eTh) , Gabal Gattar area, North Eastern Desert, Egypt.

The equivalent **(eTh/k)** contour map (Figure 13) is divided into three levels of thorium concentrations. The lowest level associated mainly with hammamat sediments and having values less than 2.3. The intermediate level ranged from 2.9 to 6.9 and recorded over pink granite , granodioritic and metavolcanics. The highest level (more than 7.1) is related to red granite.

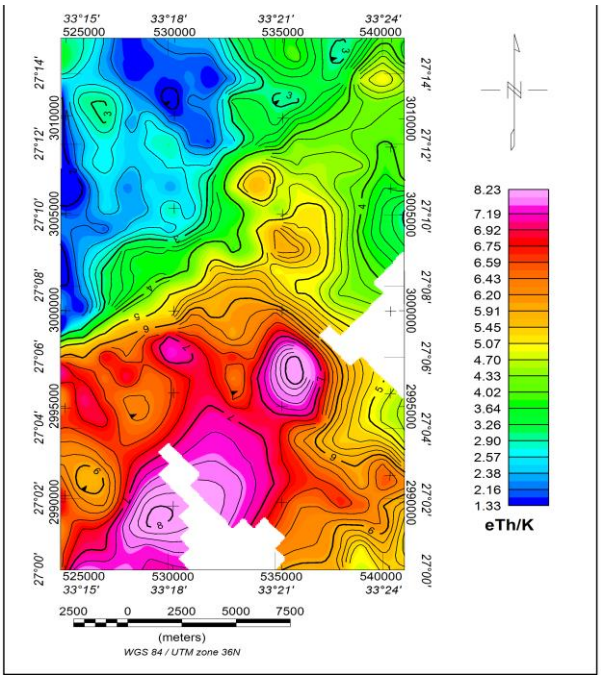

Fig. (13): Fill coloured contour map of equivalent (eTh/k) , Gabal Gattar area, North Eastern Desert, Egypt.

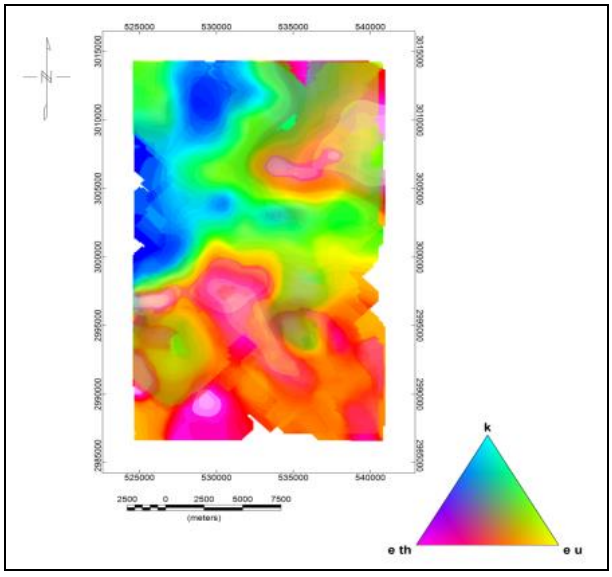

Fig. (14): False color absolute radioelements composite image, Gabal Gattar area, North Eastern Desert, Egypt.

According to J. S. Duval, the interpretation of aerial radiometric data can be deeply enhanced through the use of composite-color images. These images are produced by assigning one of three basic colors (red, green, blue) to each of three radiometric parameters. Although the basic measurement gives only three parameters—potassium (K), uranium (U), and thorium (Th)—the use of ratios gives nine different radiometric

Parameters—U, K, Th, U/Th, U/K, Th/K, Th/U, K/U, and K/Th. These nine parameters can be combined

three at a time to produce five convenient composite-color images.

An element image, which combines U, K, Th, that tends to reveal the lithology.

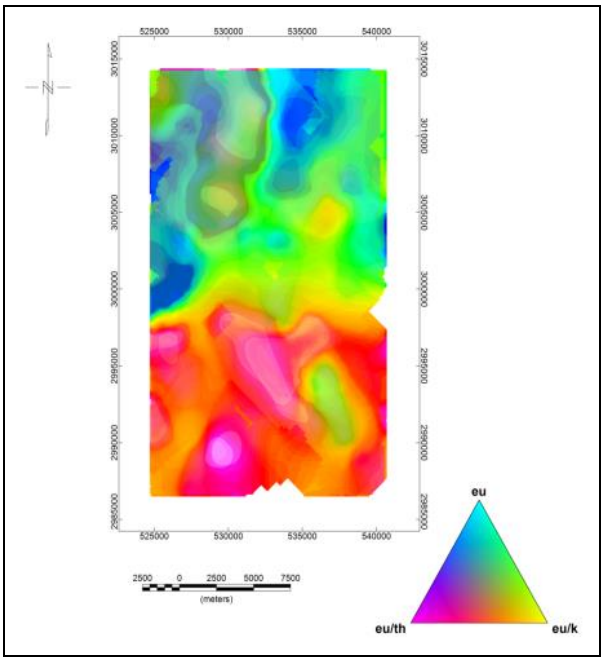

Fig. (15): False color equivalent uranium composite image , Gabal Gattar area, North Eastern Desert, Egypt.

A uranium image, which combines U, U/Th, and U/K, that emphasizes uranium and highlights areas of potential uranium mineralization.

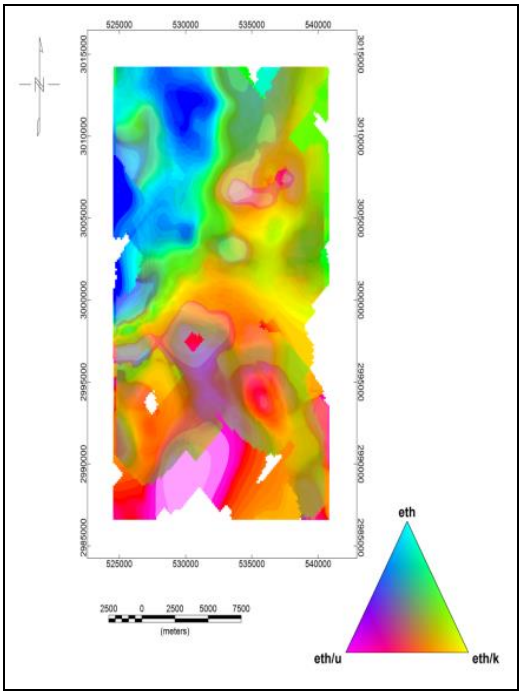

Fig. (16): False color equivalent thorium composite image, Gabal Gattar area, North Eastern Desert, Egypt.

A thorium image, which combines Th, Th/U, and Th/K, that emphasizes areas of relatively high thorium content.

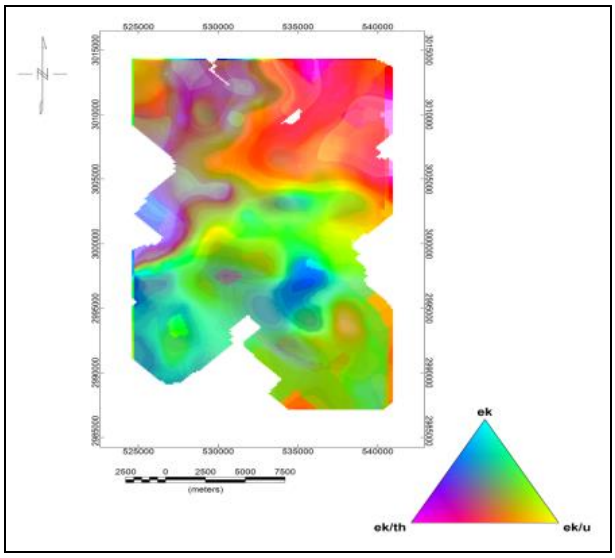

Fig. (17): False color potassium composite image , Gabal Gattar area, North Eastern Desert, Egypt.

A potassium image, which combines K, K/Th, and K/U, that emphasizes areas of relatively high potassium content.

Quantitative Interpretation

The quantitative interpretation depends principally upon the fact that, the absolute and relative concentrations of the radioele-ments (K, eU and eTh) differ measurably and significantly with lithology (Darnley and Ford, 1989). The quantitative treatment of

The spectrometric data in the present study is discussed in a statis-tical framework. The collected spectrometric data (T.C, eU, eTh andK) are in the form of digital grids. Standard statistics were applied to the raw data to calculate means, minima, maxima, standard deviations and coefficient of variability (CV%) technique for each variable (Table 1). The statistical analysis was applied on the four variables (T.C, eU, eTh, K of each rock unit, according to the detailed geologic map of the study area. Table 2 summarize the statistical results of the four variables, as well as the three ratios over the rock units in the area under investigation.

For a certain variable value in the study area, if the coefficient of variability in percent (CV%) is less than 100%, the variables tend to exhibit normal distribution,

according to the following Eq. (1):

$$CV\ \% = (S / X) \times 100$$

where:

S is the standard deviation and X is the arithmetic mean.

ROCK UNIT	COLOR	VARIABLE	MIN	MAX	X	S	CV	X+S	X+2S	X+3S
HAMMAMAT SEDIMENTS	BLUE	K (%)	4.7	15.4	11.4	4.7	40.9	16	20.7	25.4
		eU(ppm)	0.01	20.8	13.4	9.3	69.3	22.6	31.9	41.1
		eTH(ppm)	6.3	42.2	27.8	15.6	56.1	43.4	59	74.5
		eU/K	0.01	1.13	0.8	0.5	67	1.3	1.8	2.3
		eU/eTH	0.01	0.32	0.23	0.14	64.4	0.4	0.5	0.7
		eTH/K	1.3	2.6	2.11	0.55	25.9	2.7	3.2	3.7
		TC	9.1	49.5	35	17.9	51.2	52.8	70.6	88.5
PINK GRANITE	GREEN	K (%)	16.7	20.8	18.8	1.6	8.6	20.4	22	23.6
		eU(ppm)	23.7	36.3	29.5	4.9	16.7	34.4	39.3	44.3
		eTH(ppm)	50.6	105	79	21.6	27.5	100	122	144
		eU/K	1.24	1.61	1.4	0.14	10	1.6	1.7	1.8
		eU/eTH	0.34	0.41	0.38	0.03	7.6	0.41	0.44	0.46
		eTH/K	2.9	4.33	3.6	0.6	15.8	4.2	4.8	5.3
		TC	57.5	87	73	11.7	16	84.9	96.6	108
GRANODIORITIC AND GREY GRANITE	YELLOW	K (%)	21.8	23.9	22.8	0.92	4	23.8	24.7	25.6
		eU(ppm)	40	60	49	8.6	17.5	57.6	66.2	74.8
		eTH(ppm)	113	136	125	9.5	7.6	134	144	153
		eU/K	1.8	2.6	2.2	0.34	15.6	2.5	2.9	3.2
		eU/eTH	0.43	0.46	0.45	0.01	2.9	0.46	0.47	0.48
		eTH/K	4.7	5.9	5.3	0.52	9.8	5.8	6.3	6.8
		TC	92.7	109	101	7.2	7.1	108	115	123
METAVOLCANIC	RED	K (%)	24.6	28.6	26.4	1.6	6.1	28	30	31
		eU(ppm)	65.4	76.6	71.4	4.4	6.14	76	80	85
		eTH(ppm)	142.5	166	155	9.3	6.02	164	173	183
		eU/K	2.8	3.3	3.1	0.2	6.3	3.3	3.5	3.7
		eU/eTH	0.5	0.6	0.51	0.04	7.5	0.55	0.59	0.63
		eTH/K	6.2	6.9	6.6	0.3	4.2	6.86	7.14	7.42
		TC	113	129	121	6.5	5.4	128	134	141
RED GRANITE	PINK	K (%)	30.2	35.8	33	4	11.9	37	41	45
		eU(ppm)	81	100	90	13	14.9	104	117	131
		eTH(ppm)	175	207	191	23	12	214	237	261
		eU/K	3.4	9.5	4	0.8	19.4	4.7	5.5	6.3
		eU/eTH	0.63	1.1	0.9	0.4	40.2	1.2	1.6	2
		eTH/K	7.2	8.2	7.7	0.74	9.5	8.4	9.2	10
		TC	134	164	149	21	13.9	170	190	211

Environmental impacts

The radiation exposure rate was calculated by applying the following expression (IAEA, 1991): **Exposure rate** (**μRhr−1**)=**1.505K** (**percent**)+**0.653 eU** (**ppm**)+**0.287 eTh** (**ppm**)

The radiation exposure rate can be converted to equivalent radiation dose rate (RDR) as follows (IAEA 1979):

Dose rate (**mSv yr−1**)=**0.0833∗exposure rate**(**μRhr−1**)

On the other hand, the variations in uranium and thorium ratios reflect the extent of U migration in or out of this environment. The migration rate of uranium could be calculated according to Eqs. (2) and (4).

According to the(NMA) nuclear materials authority Internal Scientific Report (1999), the uranium migration value (Um for a certain rock unit can be obtained by subtracting the original uranium content (U0) from the present measured uranium content Up, as shown through the following steps:

A- The paleo-uranium background (i.e. original uranium contentU0) can be calculated, using the equation:

U0 = eTh – (eU/eTh)

where eTh is the average eTh content (in ppm) in a certain geo-logic unit and eU/eTh is the average regional eU/eTh ratio for dif-ferent geologic units.

The amount of mobilized uranium (i.e. amount of uranium migration, Um), can be calculated, using the equation:

Um = Up - U0

where Up is the average uranium content in a certain geologic unit. A positive Um value means inward uranium migration (mobility), whereas a negative value of Um indicates an outward uranium migration.

DOSE RATE	MINIMUM *(mSv/y)*	MAXIMUM *(mSv/y)*	MEAN *(mSv/y)*
HAMMAMAT SEDIMENTS	0.79	4.41	3.05
PINK GRANITE	5.01	7.96	6.5
GRANODIORITIC	8.55	10.61	9.54
METAVOLCANIC	11.24	13.119	12.188
RED GRANITE	13.816	16.6	15.208

ILRU	Uo (ppm)	UP (ppm)	Um (ppm)	P (%)
HAMMAMAT SEDIMENTS	27.565	13.365	-14.2	-106.247
PINK GRANITE	78.394	29.51	-48.884	-165.65
GRANODIORITIC	124.075	49.0225	-75.0525	-153.098
METAVOLCANIC	154.278	71.42	-82.858	-116.015
RED GRANITE	190.165	90.42	-99.745	-110.3129

There are two statuses of (Um) values; the first if Um > 0, it reflects that uranium migration is into the geologic body, the sec-ond is if Um < 0, it reflects that uranium migration is out of the geologic body.

The mobilized Uranium migration rate p% can be calculated, using the equation:

$$P = (Um / Up) \times 100$$

AERO-MAGNERIC SURVEY

General

Total Magnetic Intensity

The total magnetic intensity is the vector resultant of the intensity of the horizontal and vertical components of the Earth's magnetic field at a specified point.

Magnetic anomaly is a local variation in the Earth's magnetic field resulting from variations in the chemistry or magnetism of the rocks. Mapping of variation over an area is useful in detecting structures hidden by overlying material.

Residual is what remains after regional magnetic trends are removed from the total intensity Residual maps show local magnetic variations, which may have exploration significance.

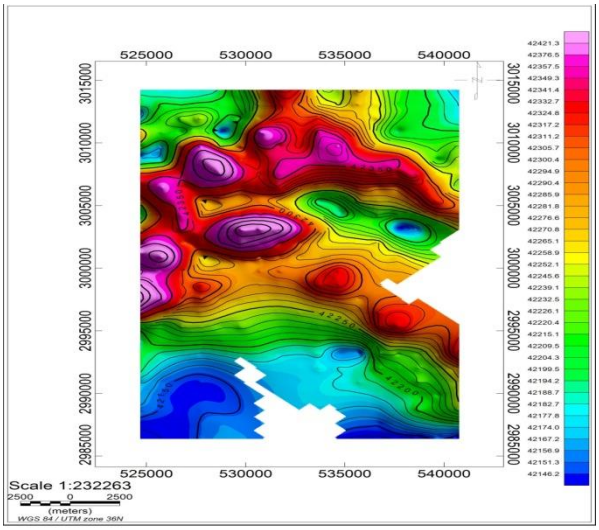

Fig. (18): Total Magnetic Intensity Map, Gabal Gattar area, North Eastern Desert, Egypt.

Reduction To The Pole

Reduction To The Pole (**RTP**) is a standard part of **magnetic** data processing method, especially for large-scale mapping. **RTP** operation can transform a **magnetic** anomaly caused by an arbitrary source into the anomaly that the same source would make if it is located at the pole and magnetized by induction only.

Removing the dependence of magnetic data on the magnetic inclination, i.e., converting data that have been recorded in the inclined Earth's magnetic field to what they would have looked like if the magnetic field had been vertical. Reduction to the pole eliminates anomaly asymmetry caused by inclination and locates anomalies above the causative bodies, assuming that the remanent magnetism is small compared to the induced magnetism. It is difficult to do at low magnetic inclinations, in which case reduction to the equator is preferred.

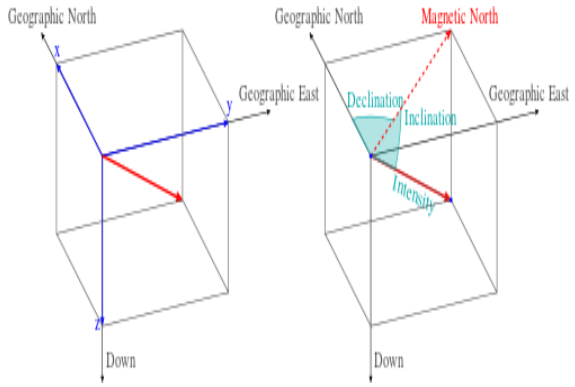

Intensity of the field is often measured in gauss (G), but is generally reported in nanoteslas (nT), with 1 G = 100,000 nT.

The Inclination is given by an angle that can suppose values between -90° (up) to 90° (down). In the northern hemisphere, the field points downwards. It is straight down at the North Magnetic Pole and rotates upwards as the latitude decreases until it is horizontal (0°) at the magnetic equator. It continues to rotate upwards until it is straight up at the South Magnetic Pole. Inclination can be measured with a dip circle.

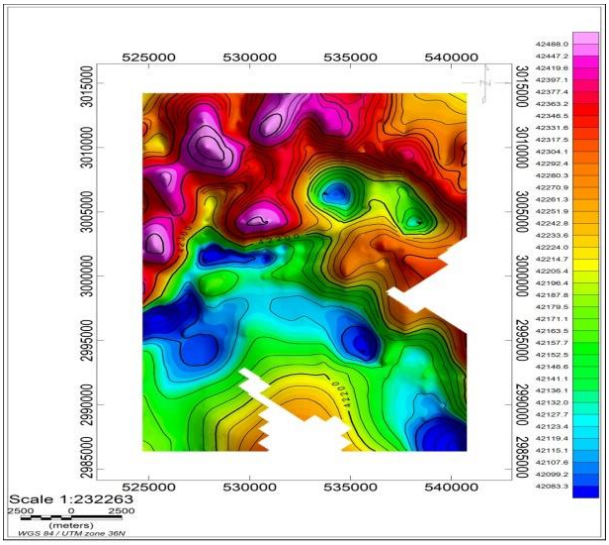

Fig. (19): Reduction To the magnetic Pole Map, Gabal Gattar area, North Eastern Desert, Egypt.

Magnetic declination, sometimes called **magnetic** variation, is the **angle** between **magnetic** north and true north. As the earth's **magnetic** field changes over time, the positions of the north and south **magnetic** poles gradually change.

Edge Detection Methods

Various techniques are concerned with the detection of the edges of potential field anomalies generated by geological structures. Currently, edge detectors constitute an essential step in the process of potential field data interpretation. The total horizontal derivative (THDR) method has been used widely to map the boundaries of susceptibility contrasts. It exploits the fact that the horizontal derivative of the RTP magnetic field generated by a tabular body tends to have maximum values over the edges of the anomalous body in case the edges are vertical and well-separated from each other .

THDR is not only less susceptible to the noise in the data, but also strong in detection of shallow magnetic sources . It has high amplitude over the edge of the magnetic source.

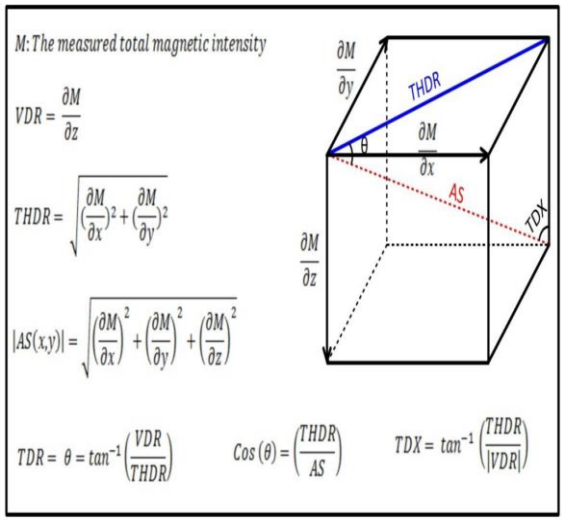

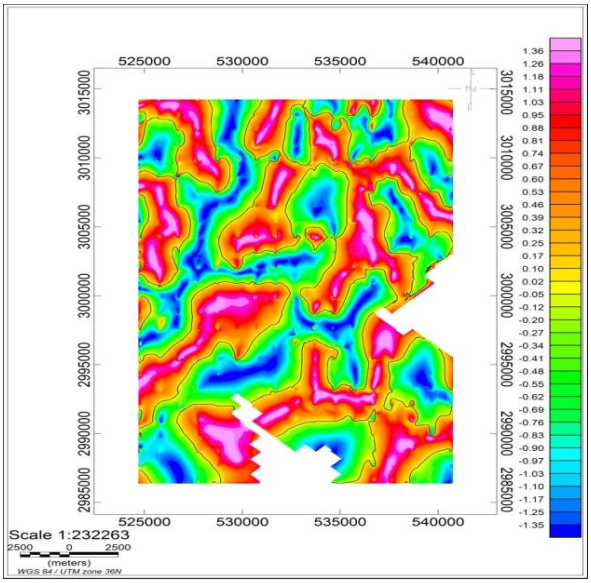

Fig. (20): TDR MAP, Gabal Gattar area, North Eastern Desert, Egypt.

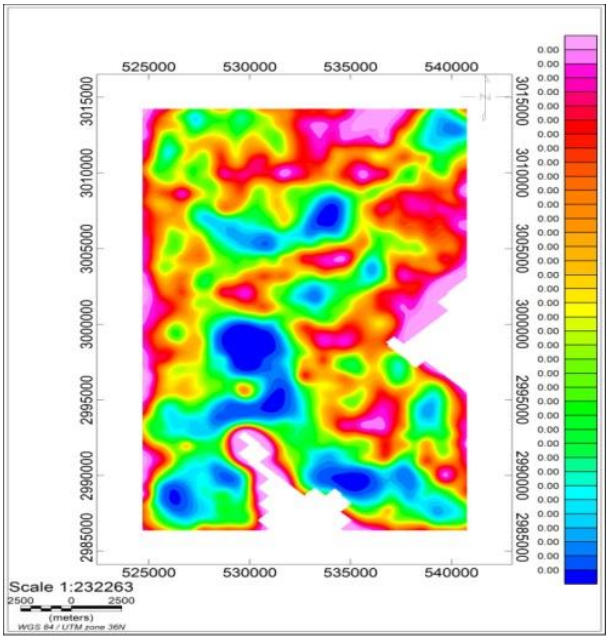

Fig. (21): UP-Con of HD-TDR, Gabal Gattar area, North Eastern Desert, Egypt.

Euler Deconvolution

The Euler Deconvolution is an automatic method used for locating the source of potential fields based on both their amplitudes and gradients. So, it is used to locate the structures and depths at contact locations.

The method was developed by Thompson (1982) to interpret 2D magnetic anomalies and extended by Reid *et al.* (1990) to be used on grid-based data.

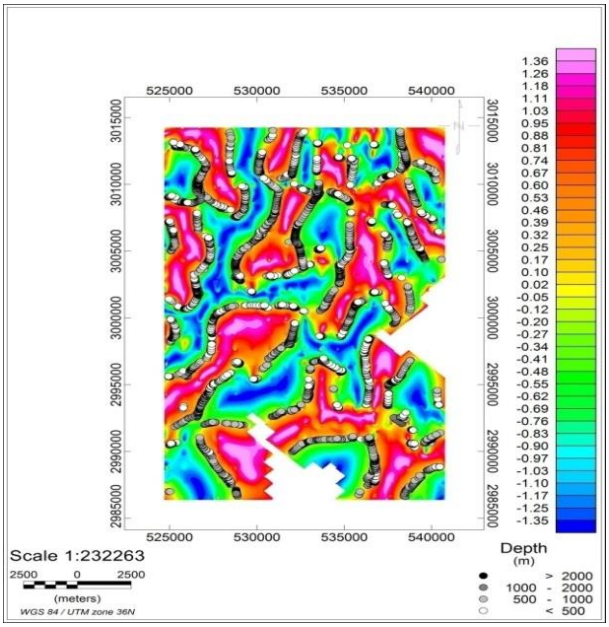

TDR- Fig. (22): ED-ST-0, Gabal Gattar area, North Eastern Desert, Egypt.

The Power Spectrum

To split the regional and residual components of the magnetic data, the two dimensional power spectrum was calculated from the total intensity magnetic map . The calculated power spectrum illustrates two linear segments, associated to the residual and regional components.

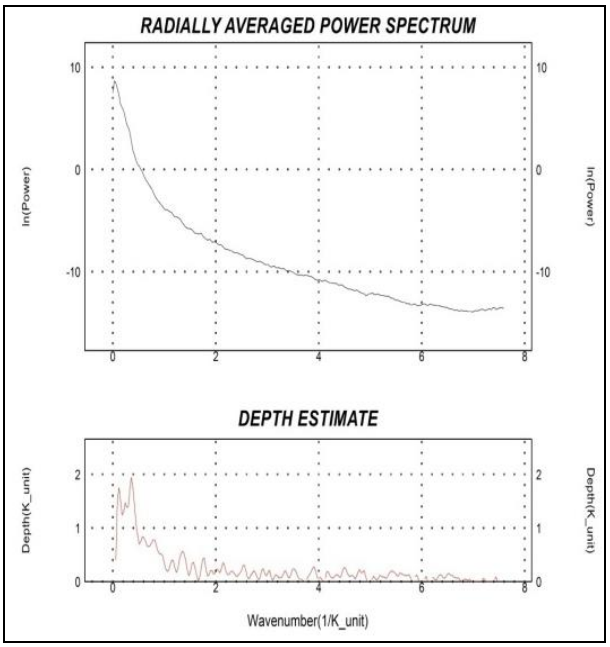

Depth = - slope /4π

For regional

Slope = (y2 _ y1) /(x2 _ x1)

Slope = (9 _ 0) / (0.7 _ 0)

Slope = 12.85

Depth = 1.02 km

For residual

Slope = -2 _ (-10) /(3_0)

Slope = 2.6

Depth = 0.2

Depth estimation

Regional 1.2 km

Residual 0.3km

Graphical method in depth evaluation only applied on positive anomalies.

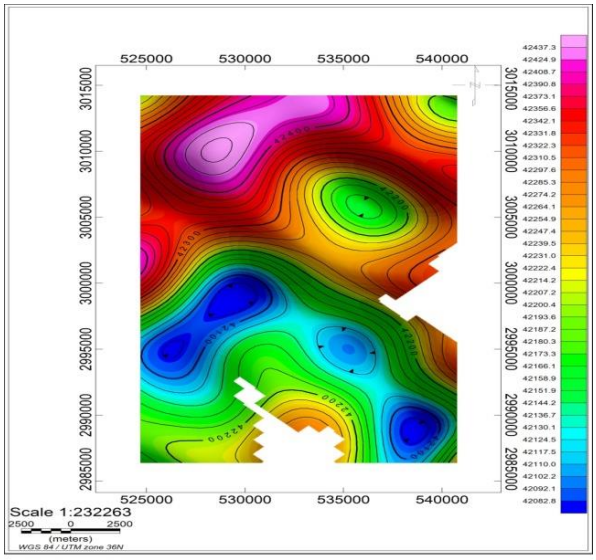

Fig. (23): Regional Map, Gabal Gattar area, North Eastern Desert, Egypt.

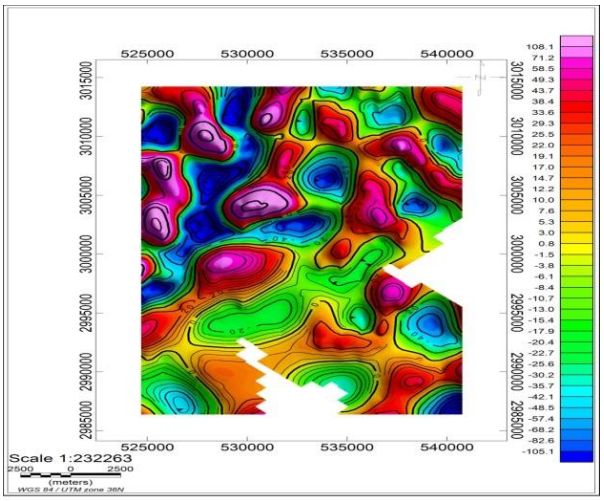

Fig. (24): Residual Map, Gabal Gattar area, North Eastern Desert, Egypt.

Residual Map Report

The map has two parts:

Northen part has high anomalies , some anomalies are circles and others are oval in shape , there is a small anomaly inside high anomaly it is trending to NE . the northen part is characterized by high anomalies ,The high anomalies in the north have N_S trend with circular shape.

Southern part has small anomalies trending NE direction .

- There is a small anomaly which has NE direction with irregular shape between the south and the north parts, There is also a high gradient which indicates a possible presence of fault.
- Map values are generally medium but is subdivided by value into high , medium and low anomalies along map .
- Gradient along map is generally medium but it gets obviously high gradient at high anomalies .
- We have a large medium anomaly that is continous almost along map plane , it dips in northwest direction which indicates fault plan direction to be northeast.
- Shape of anomalies are generally oval to circular indicating presence of dykes.

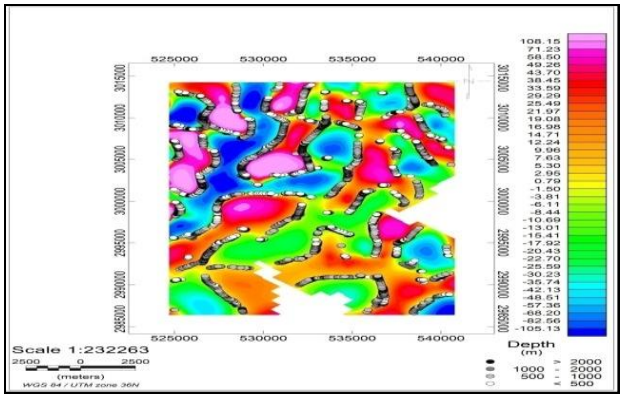

Fig. (25): RES-ED-ST-0, Gabal Gattar area, North Eastern Desert, Egypt.

Horizontal Gradient

The horizontal gradient magnetic anomaly map has been set from the RTP land magnetic intensity anomaly map using Oasis Montaj (1998). The energy in the high frequency region, which largely consists of noises, and contribution from the near surface magnetic sources, is greatly increased. Although, the horizontal derivative is a nonlinear operation that cannot be described in terms of a linear filter, it is claimed to define a sharp contact between two rock types having different magnetization (Stanley, 1976). Such situation may occur in the faulted parts, where block displacements bring lithologies of different magnetizations to the same depth level on both sides of a fault plane.

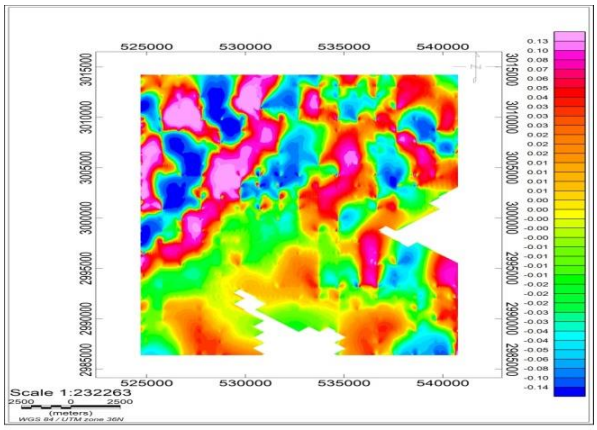

Fig. (26): HG-X, Gabal Gattar area, North Eastern Desert, Egypt.

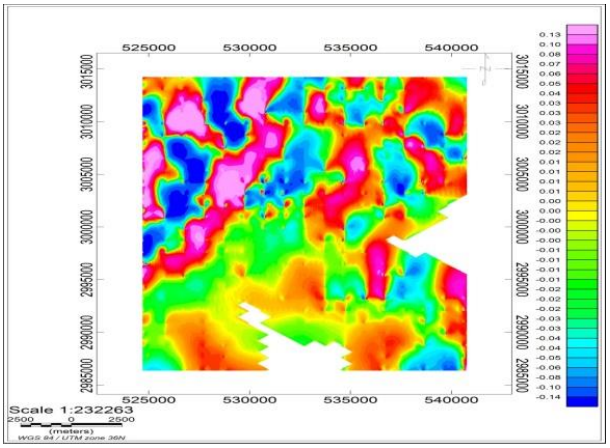

Fig. (27): HG-Y, Gabal Gattar area, North Eastern Desert, Egypt.

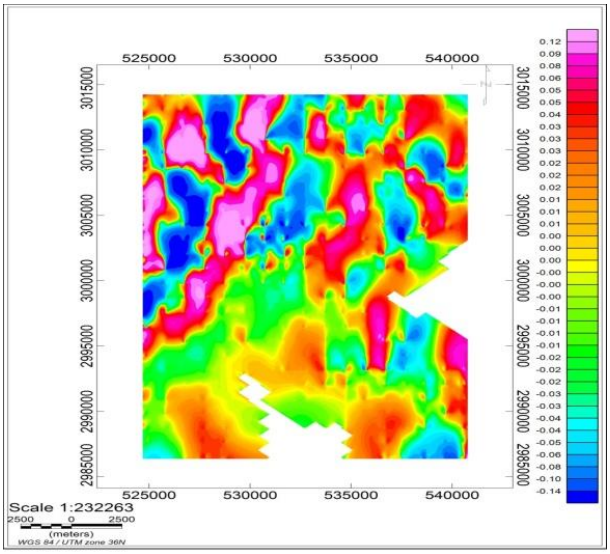

Fig. (28): THG, Gabal Gattar area, North Eastern Desert, Egypt.

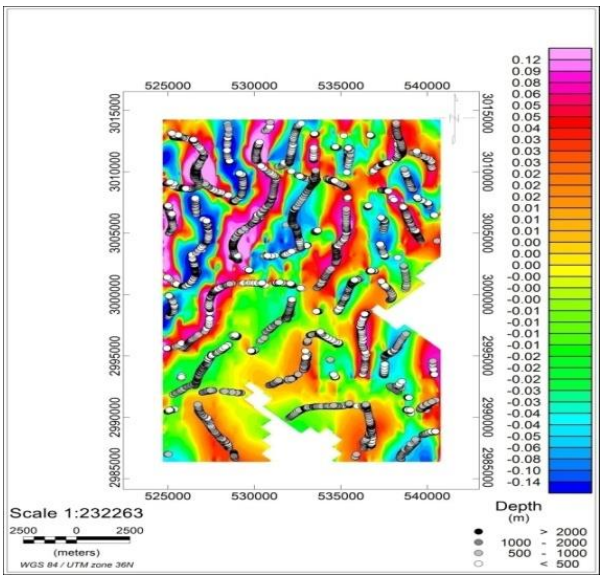

Fig. (29): THG-ED-ST-0, Gabal Gattar area, North Eastern Desert, Egypt.

Second Verticle Deravative (SVD) OF RTP

In geophysics, derivative maps are maps of one of the derivatives of a potential field, such as the Earth's gravity or magnetics. The more common derivative maps are those of the second vertical derivative (second-derivative map), which strongly improve the morphology of the maps and so a more accurate location of the anomalies.

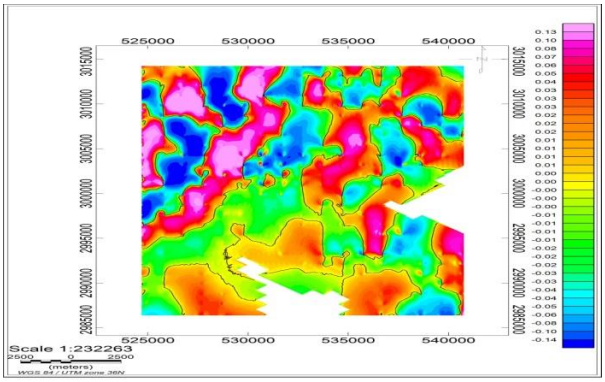

Fig. (30): SVD, Gabal Gattar area, North Eastern Desert, Egypt.

CONCLUSION

The mode of distribution of uranium mineralization in Gabal Gattar district is controlled by three types of traps. Within granite faults, composite and basic dike traps are the identified types in the study area. In the first two traps, the uranium mineralization is present in lenses that vary in size and uranium grade from trap to another. The basic dike trap acted as a brrier for localization of high uranium mineralization at its contact zone with granite. The effect of hydrothermal activities and tectonic role are clear in controlling the distribution of uranium mineralization in Gabal Gattar district.

The most important uranium mineralization lenses are localized in the Northern zone of G. Gattar granite and along the contact zone of the granite with the Hammamat sediments along a reverse fault following ENE-WSW direction, the intensity and concentration of uranium increased when this contact fault zone is interrupted by NW-SE and NNE-SSW faults.

Gabal Gattar district can be considered as a potential for the presence of small to medium scale uranium deposit. It needs detailed drilling works to define the ore zones boundaries and to be able to estimate uranium reserves and performing the feasibility study.

REFERENCES

Abd El Hadi, H.M. (1978): Aeroradiometric data and its relation to the regional geology of Bakriya area, Eastern Desert (Corroborated with aeromagnetic Survey) Ph.D. Thesis, Faculty of Science, Cairo University, Egypt, 259 p.

Abd El-Nabi, S.H. (1995): Nature of sedimentation and uraniferous provinces verified by airborne gamma-ray spectrometry. E Qena, Egypt. J. Sedimentology Society of Egypt, Vol.3, pp. (63-71).

Abd El-Nabi, S.H. (2012): An analysis of airborne gamma ray spectrometric data of Gabal Umm Naggat Granitic Pluton, central Eastern Desert, Egypt. JAKU: Earth Sci., 23(2), p.p. 19-42, DOI: 10.4197 / Ear. 23-2.2.

Abdel Aziz, M.G. (1968): The geology of Wadi Kareim area, Ph.D. Thesis, Cairo Univ.

Abdel Gawad, A. (1969): New evidence of transcurrent movement in Red Sea area and petroleum implications. American Assoc. Pet. Geol., Bull. 33, 53, pp. (14661479).

Abdel Meguid, A.A. (1986): Geologic and radiometric studied of uraniferous granite in Um Ara Um Shilman area, South Eastern Desert, Egypt. Ph.D. Thesis, Suez Canal Univ., 222 p.

Abu El Saadat, M.M. (2009): Arab mining society, Special issue on theEgyptian Iron Ores, Cairo, pp 20–28.

Abuelnaga, H.S.O. (1998): Exploration for radioactive minerals in wadiMuweylhahwadiBayzah area using aerospectrometric and aeromagnetic survey data, South Eastern desert, Egypt. PH.D. Thesis, Ain shams Univ., 286 p.

Aero Service (1983): Training course in airborne magnetic and radiometric surveying, presented to the Egyptian General Petroleum Corporation, Cairo, Egypt.

Aero-Service (1984): Final operational report of airborne magnetic radiation survey inthe Eastern Desert, Egypt for the Egyptian General Petroleum Corporation. AeroService, Houston, Texas, Six Volumes.

Affleck, J. (1963): Magnetic anomaly trend and spacing patterns. Geophysics, V.28. No. to 3, pp. (378-395).

Akaad, M.K. and A. Noweir (1980): Geology and Lithostratigraphy of the Arabian Desert Orogenic belt of Egypt between lat. 250 35' and 260 30'N. Bull. Inst. Applied Geol., King Abdul Aziz Univ., Jeddah 3(4): pp. 127-135.Moghazi AM, Ali KA, Wilde SA, Zhou Q, Andersen T, Andresen A,

Akaad, M.K. and M.A. Essawy (1964): The meta-babbrodiorite complex NE of Gabal Atud, Eastern Desert, Egypt and the term "epidiorite". Bull. Sci. Techn., Assiut Univ. 7: pp. 83-108.

Ammar, A.A. (1973): Application of aerial radiometry to the study of the geology of Wadi El Gidami area, Eastern Desert, Egypt (with aeromagnetic application). Thesis, Ph.D., Cairo Univ., Egypt, 424 p.

Ammar, A.A. and Rabie, S.I. (1991): Application of geophysical techniques to the interpretation of aeromagnetic survey data, South Eastern Desert, JKAU Science ..Earth Science 4 pp (67–103).

Bentor, Y.K. (1985): The crustal evolution of the Arabo-Nubian Massif with special reference to the Sinai Peninsula. Precambr Res 28:1–74.